maintained acceptable abilities in power gain, noise figures, and IIP3 performances.

ACKNOWLEDGMENTS

The authors acknowledge the fabrication support provided by Taiwan Semiconductor Manufacturing Company (TSMC) through the National Chip Implementation Center (CIC) and also appreciate to the CIC for high-frequency measurement under the assistance by Green Technology Research Center, Chang Gung University.

REFERENCES

1. X. Guan and C. Nguyen, Low-power-consumption and high-gain CMOS distributed amplifiers using cascade of inductively coupled common-source gain cells for USB systems, IEEE Trans Microwave Theory Tech 54 (2006), 3278–3283.
2. M.M. Green, M.B. Pisani, and C. Dehollain, Design methodology for CMOS distributed amplifiers. In Proceedings of the IEEE International Symposium on Circuits and Systems, ISCAS 2008, Seattle, WA, May 2008, pp. 728–731.
3. R.C. Liu, C.S. Lin, K.L. Deng, and H. Wang, Design and analysis of DC-to-14-GHz and 22-GHz CMOS cascade distributed amplifier, IEEE J Solid-State Circuits 39 (2004), 1370–1374.
4. F. Zhang and P. Kinget, Low power programmable-gain CMOS distributed LNA for ultra-wideband applications, In Proceedings of the Symposium on VLSI Circuits Digest of Technical Papers, 2005, pp. 78–81.
5. C.W. Kim and M.S. Kang, An ultra-wideband CMOS low noise amplifier for 3–5-GHz UWB system, IEEE J Solid-State Circuits 40 (2005), 544–547.
6. A. Bevilacqua and A.M. Niknejad, An ultra-wideband CMOS low-noise amplifier for 3.1–10.6-GHz wireless receivers, IEEE J Solid--State Circuits 39 (2004), 2259–2268.
7. C.H. Wu, C.H. Lee, W.S. Chen, and S.I. Liu, CMOS wideband amplifiers using multiple inductive-series peaking technique, IEEE J Solid-State Circuits 40 (2005), 548–552.
8. B.M. Ballweber, R. Gupta, and D.J. Allstot, A fully integrated 0.5–5.5 GHz CMOS distributed amplifier, IEEE J Solid-State Circuits 35 (2000), 231–239.
9. R.E. Amaya, N.G. Tarr, and C. Plett, A 27 GHz fully integrated CMOS distributed amplifier using coplanar waveguides, IEEE RFIC Symposium, Digest of Papers, Fort Worth, TX, June 2004, pp. 193–196.
10. R.C. Liu, C.S. Lin, K.L. Deng, and H. Wang, A 0.5–14-GHz 10.6-dB CMOS cascode distributed amplifier, In Proceedings of the VLSI Symposium, 2003, pp. 139–141.
11. M.D. Tsai, K.L. Deng, H. Wang, C.H. Chen, C.S. Chang, and J.G.J. Chern, A miniature 25-GHz 9-dB CMOS cascaded single-stage distributed amplifier, IEEE Microwave Wireless Compon Lett 14 (2004), 554–556.
12. Y.-J. Wang and A. Hajimiri, A compact low-noise weighted distributed amplifier in CMOS, In Proceedings of the IEEE International Solid-State Conference, Digest Technical Papers, ISSCC 2009, San Francisco, CA, May 2009, pp. 220–222.

DESIGN AND EXPERIMENTAL EVALUATION OF A COMPOSITE STRAIN ROSETTE USING FIBER BRAGG GRATING

C. A. Ramos,[1] R. de Oliveira,[2] A. T. Marques,[4] and O. Frazão[3]

[1] Instituto Superior de Engenharia do Porto (ISEP), Departamento de física (DEFI), Rua Dr. António Bernardino de Almeida 431, 4200-072, Porto, Portugal
[2] Instituto de Engenharia Mecânica e Gestão Industrial (INEGI), Composite Material and Structures Unit (UMEC), Rua Dr. Roberto Frias, 400 4200-465 Porto, Portugal; Corresponding author: rcosta@inegi.up.pt
[3] INESC Porto, Rua do Campo Alegre 687, 4169-007 Porto, Portugal
[4] Faculdade de Engenharia da Universidade do Porto (FEUP), Departamento de Engenharia Mecânica e Gestão Industrial (DEMEGI), Rua Dr. Roberto Frias, s/n 4200-465 Porto, Portugal

Received 5 November 2010

ABSTRACT: *The purpose of this study is to design a composite strain rosette using embedded fiber Bragg grating (FBG) sensors. Those strain rosettes are meant to be used as alternative to the conventional electric rosettes in structural health monitoring applications being glued at the structure surface. A thin (400 μm) and flexible weaved carbon fiber reinforced plastic (CFRP) composite rosette is proposed. The three FBG sensors were written in a single optical fiber. Special care was devoted to the embedding process of the optical fiber sensors in the weaved composite plate in order to avoid significant alteration of the light reflected back by the FBG. The strain response of the composite rosette was compared to electrical strain gage's when applied at the surface of an aluminium sample submitted to tension, flexion and to dynamic strain.* © 2011 Wiley Periodicals, Inc. Microwave Opt Technol Lett 53:1853–1857, 2011; View this article online at wileyonlinelibrary.com. DOI 10.1002/mop.26098

Key words: *optic fiber sensor; fiber bragg grating; composite material; strain measurement; structural health monitoring*

1. INTRODUCTION

Strain monitoring is a commonly used method for structural health monitoring (SHM). The strain information is used to verify design assumptions about loading patterns or can be combined with long term models to predict structure residual life.

The rosette configuration is extensively used in experimental stress analysis to measure the state of strain (i.e., the two principal strains and their directions) at a point on the surface. They substitute single-arm strain gauges whenever the geometric and/or load complexity prevent any a priori knowledge of the axes of orientation [1].

Classical electrical strain gages (SGs) rosettes consist of metallic foils sealed in a polyimide film. However, they are not the best solution for long term SHM due to their week creep and fatigue behavior, sensor debonding being commonly observed.

Optical fiber sensor based rosettes have been developed as alternative to the electrical SGs rosettes [1–7]. Two types of optical fiber sensors have been successfully used: the Fabry-Pérot [1–3] interferometer and the FBG [4–7]. Valis et al. [1] developed a rosette based on intrinsic Fabry-Pérot interferometers. They achieved performance comparable with an electrical strain rosette when optical fiber sensors are glued at the surface of the structure. If directly embedded in unidirectional laminates (graphite/PEEK) subjected to uniaxial stress applied along the central rosette arm direction [2], they observed a satisfying behavior of their sensors. Case et al. [3] chose the extrinsic Fabry-Pérot interferometers configuration. They embedded them in graphite/epoxy laminates and verified their effectiveness in measuring arbitrary strain states within the laminates in the axial (0°) and transverse (90°) direction. Some discrepancies were however noticed at 45°. They also observed a significant decrease in the composite laminate compressive strength due to the presence of the embedded sensors.

Compared with these two sensors, FBG have the advantage to be easily multiplexed. This permits to monitor simultaneously the strain in three directions using a single optical fiber by assigning each sensor to a different portion of the optical

spectrum. The French technological research organisation CEA developed and commercialises FBG strain rosette encapsulated in a polyimide film [4] to be glued at the structure surface. This rosette is based on three temperature auto-compensated sensors. The weak point of this encapsulated rosette as mentioned previously remains the insufficient long term properties of the polyimide films. Haran et al. [5] proposed a rosette with a similar shape (i.e., triangular) but added a fourth FBG for temperature compensation. The temperature measuring FBG has to be bonded in such a way that it experiences the changes in temperature, but not the strain, to which the structure is subjected. Similar configuration has been adopted by Betz et al. [6]. They also demonstrated experimentally that the use of the backing patch produces a reduction in strain sensitivity of only around 4%. Matrat et al. [7] embedded the FBG in a composite laminate with the lay-up $[0/45_2/\text{-}45_2/90/0]_4$ corresponding to a thickness of 4.16 mm. Four different FBG were positioned at different location across the thickness and aligned with the adjacent reinforcement. The authors developed an analytical model to dissociated wavelength variation due to the strain and to the temperature. The sensor for temperature discrimination was written in an optical fiber with slightly different thermo-optical properties. Although a good accuracy in strain measurement was achieved (the largest observed error for in-plane strain component was less than 3%) the sensor embedding required the use of at least two plies of distance between sensors to decrease the neighbouring effect of optical fiber s on sensors responses.

In this article, the embedding in a thin CFRP composite patch is considered. This will permit the increase of the long term properties of the strain rosette and its range of application (i.e., in more critical environments). Similar composite patches based on a single embedded FBG are commercially available for longitudinal strain measurement. Smartfibers commercialises apodised FBG sensor embedded in glass fiber reinforced plastic patches [8] having nominal dimensions of 120×20 mm^2. FiberSensing SA commercialises uniform FBG embedded in CFRP plates [9] with dimensions of $120 \times 20 \times 9$ mm^3 that are more rigid. Both patches have significant thickness. Thinner patches are needed for less invasive sensing.

The embedding of the optical fiber sensor in a composite requires many cautions to guarantee the reliability of the information provided by the sensor. Its embedding induces stress and strain concentrations around the sensor. FBG reflection spectrum suffers some changes during the curing process due to thermal residual stresses in the case of angle-ply laminates [10–13]. In contrast, the embedding into unidirectional specimens has fewer repercussions on FBG reflection spectrum and thus on the strain measurement reliability.

It is thus normally accepted that the FBG embedment in a thick host will improve the sensor reliability [14]. It is also generally accepted that the optical fiber should be embedded between two plies of the same orientation in order to avoid the creation of a resin pocket along the optic fiber. The embedding of FBG sensors in weaved composites is rarely considered due to the complex local residual strain field promoted by the fabric weave which distorts the grating optical spectrum. In a previous study [15] the authors implemented a thin weaved composites patch with an embedded FBG for longitudinal strain monitoring.

In this article, the same CFRP weave prepregs are used for the rosette manufacturing. The rosette should achieve a good compromise, being resistant enough to significant bending and torsion displacement and inducing the less change in the structural mechanical behavior, by its reinforcement, when mounted at the surface of a structure. The rosette was applied to an aluminium specimen submitted to tensile, flexural and impact tests. The strain responses of FBG CFRP strain rosette were compared with the response of surface mounted electric strain rosette.

2. PRINCIPLE OF FIBER BRAGG GRATING SENSOR

FBG are formed when a permanent periodic variation of the index of refraction of the core is created along a section of an optic fiber, by exposing the optic fiber to an interference pattern of intense ultraviolet light [16]. The photosensitivity of silica glass permits the index of refraction in the core to be increased by the intense laser radiation. If the optical fiber with a FBG is illuminated by a broadband light source, the grating diffractive properties promote that only a very narrow wavelength band is reflected back. The centre wavelength, λ_B, of this band can be expressed by the well-known Bragg condition:

$$\lambda_B = 2n\Lambda_B \tag{1}$$

where n is the average effective index of the core and Λ_B is the grating period.

FBG sensors are wavelength-modulated sensors. Gratings are simple, intrinsic sensing elements, and give an absolute measurement of the physical perturbation it senses. Their basic principle of operation is to monitor the wavelength shift associated with the Bragg resonance condition. The wavelength shift is independent of the light source intensity. When the fiber is stretched or compressed along its axis, the period of the grating and n changes. The same is observed when the temperature fluctuates.

When embedded into a composite material, the response of a FBG sensor is dictated by the thermal strain experienced by the host material $\Delta\varepsilon_{th} = \alpha_c \Delta T$, where α_c is the coefficient of thermal expansion (CTE) of the host material and ΔT the temperature variation. In a first approximation, the Bragg equation can then be rewritten as:

$$\frac{\Delta\lambda_B}{\lambda_B} = \left\{1 + \left[\frac{1}{n}\frac{\partial n}{\partial \varepsilon}\right]_T\right\}\left(\Delta\varepsilon_{app} + \Delta\varepsilon_{th}\right) + \left[\frac{1}{n}\frac{\partial n}{\partial T}\right]_\varepsilon \Delta T = K_\varepsilon \Delta\varepsilon + \xi\Delta T \tag{2}$$

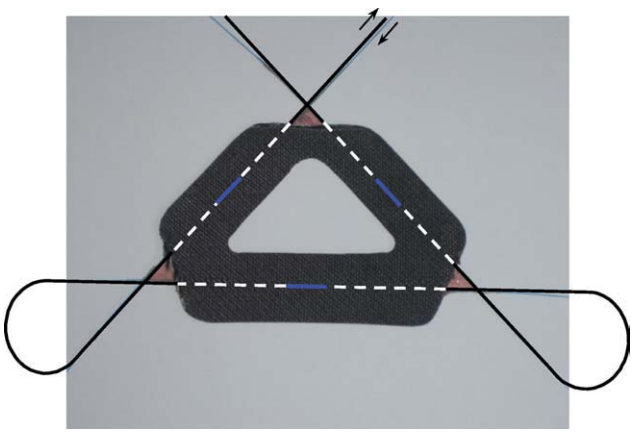

Figure 1 Composite strain rosette using Bragg sensors. [Color figure can be viewed in the online issue, which is available at wileyonlinelibrary.com]

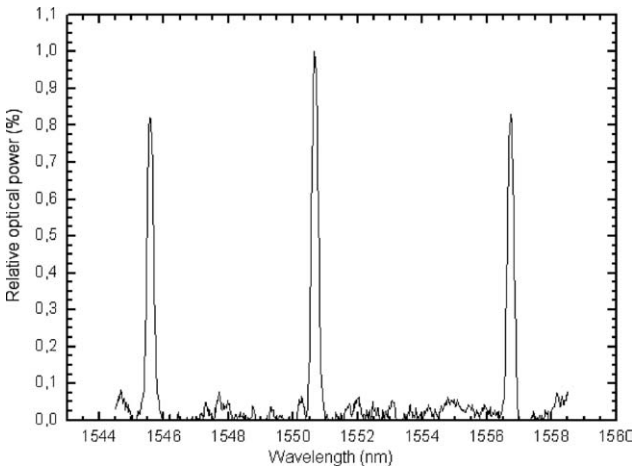

Figure 2 Spectral response of the three Bragg grating sensors

where K_ε is the sensor sensitivity to strain. $\Delta\varepsilon_{app}$ and $\Delta\varepsilon$ are the applied axial strain and the total strain transferred to the optical fiber, respectively. ξ is the silica fiber thermo-optic coefficient.

FBG sensors are sensitive to both strain and temperature. To recover the strain, it must be decoupled from the temperature variation. The temperature must then be measured separately. This can be done using a simple thermocouple or a second FBG [17].

3. CONCEPTION OF THE CFRP STRAIN ROSETTE

Nonrecoated FBG sensors 10-mm long, with a nominal resonance wavelength around 1550 nm after temperature annealing, with a strain sensitivity of $0.77 \pm 0.05.10^{-6}$ $\mu\varepsilon^{-1}$, were written in SMF – 28e® low birefringence single mode optical fiber s with an acrylate coating from Cornings.

The optical fiber has a diameter of 250 μm with coating, and 125 μm without, respectively. The coating was mechanically removed along 40 mm for grating writing as UV radiation does not penetrate through the acrylate. This last was submitted to a temperature annealing permitting its stabilization from its accelerated ageing.

Rosette design was subject of a particular attention. The resulting embedding methodology permits the embedding of FBG sensors in weaved reinforced composite laminates without distortion of the sensor reflected light.

The composite material consists of CFRP prepregs with the layer thickness of 0.20 mm, in a warp/weft 50/50 configuration (CC206 from Seal) preimpregnated by an epoxy resin (ET442). A peel-ply layer was applied at the rosette surface to control the surface roughness. This permits the improvement of the adhesion to the specimen surface at its application.

The proposed strain rosette has a delta configuration (cf. Fig. 1) having a maximal length of 90 mm and a width of 50 mm. The central part was removed providing a higher flexibility to the rosette. This rosette configuration is the same as the one that was adopted by Magne et al. [18]. It permits from only three FBG to determine efficiently the state-of-strain and provides self-temperature-compensation.

The two layers of prepegs were laid up by hand. A prestressed optical fiber was placed in the mid-plane of the laminate and positioned according to the drawing presented in Figure 1. After lay-up, the laminates were vacuum-bagged and placed in an autoclave. The material was slowly heated to 125°C under internal vacuum (0.085 MPa) and 0.1 MPa of external pressure. After holding for 2 h at this condition, the laminate was slowly cooled in the autoclave. The optical fibers were guided outside of the vacuum bag through the sealant tape. The plateau temperature was set to 125°C, which is slightly lower than the value recommended by the prepreg manufacturer (130°C). The temperature decrease guaranteed the optical fiber coating integrity. A longer plateau duration was applied to warrantee the completion of composite cure. The obtained rosette presented a final thickness of 0.4 mm.

The resulting reflection spectra of the FBG after embedding are presented in Figure 2. They reflection spectra remained narrow confirming that the FBG are not significantly affected by the transversal thermal residual stresses on the FBG sensor and any microbendings due to the weaved reinforcement.

4. EXPERIMENTAL TESTING AND RESULTS

4.1. Behavior in Tension

The CFRP rosette was applied at the surface of an aluminium sample with nominal dimensions of $305 \times 155 \times 3$ mm^3. A

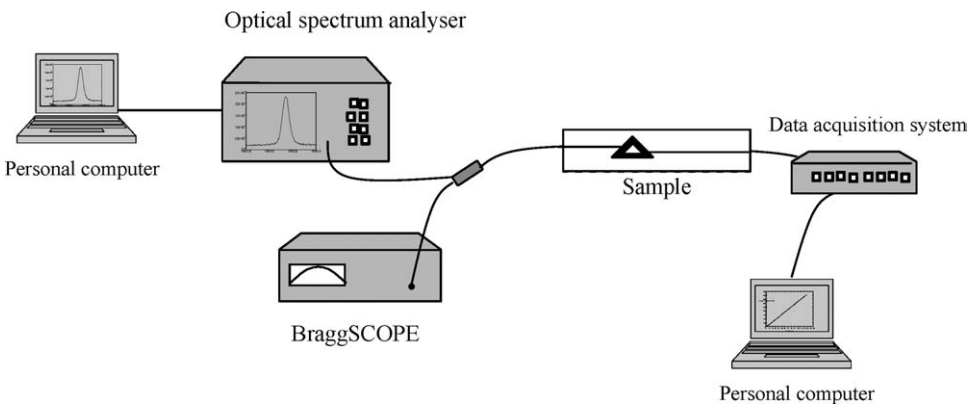

Figure 3 Experimental setup

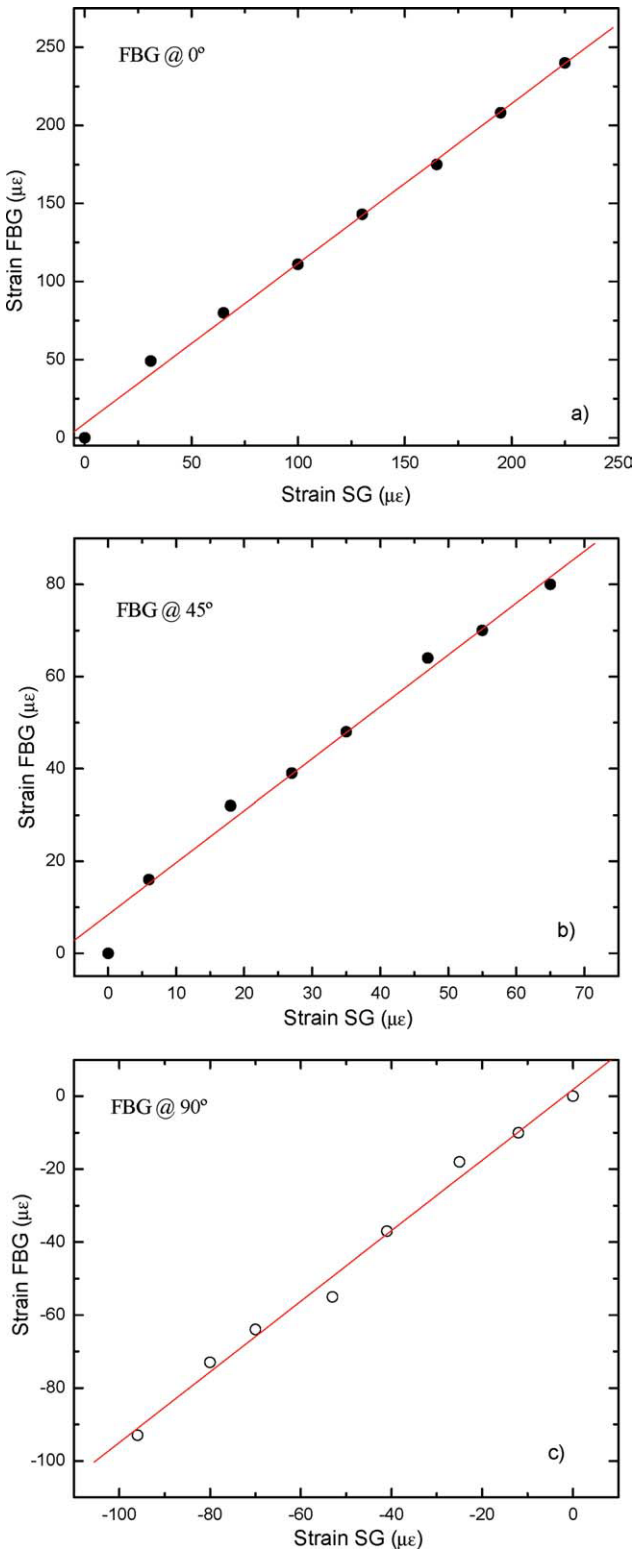

Figure 4 Analysis of the FBG sensors in three different directions. [Color figure can be viewed in the online issue, which is available at wileyonlinelibrary.com]

thin layer of a two components epoxy resin was used as adhesive. One of the FBG (0°) was positioned along the loading direction. The others were positioned at 90° and 45°, respectively.

The experimental setup (Fig. 3) used for strain measurement consisted of a BraggSCOPE FBG interrogator, from FiberSens-

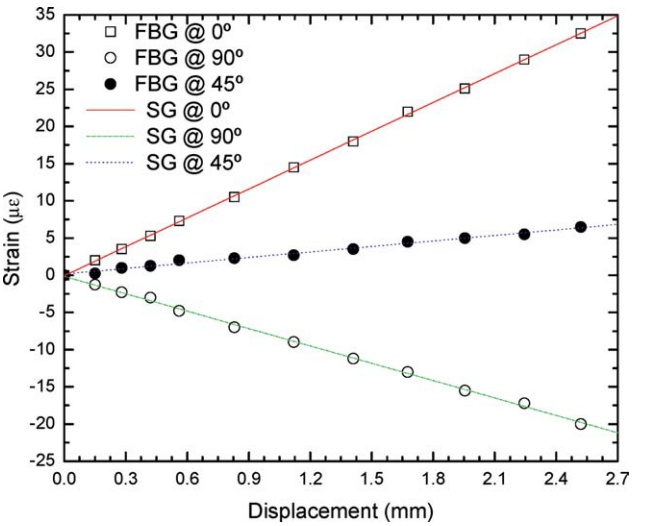

Figure 5 Comparison between the three FBG and the electric sensors. [Color figure can be viewed in the online issue, which is available at wileyonlinelibrary.com]

ing, for the Bragg wavelength shifts measurement, an AQ6330 optical spectrum analyser, from Ando, for the Bragg wavelength spectra monitoring and recording, in a personal computer, through a GPIB interface controlled by LabVIEW^{TM}. The electrical SG rosette was connected to a Spider 8 data acquisition system from HBM® linked to a computer using the Catman 3.1^{TM} software. Strain data were acquired at a sampling rate of 1 kHz.

Monotonic tensile tests were performed using an Instron® Model 4208 universal testing machine, according to the ISO 527 standard. The speed test was controlled by displacement to 1 mm.min^{-1} until a maximum load of 7 kN. In Figure 4 are presented the strain values measured by the FBG sensors in the three directions and the respective values obtained by the corresponding electrical SGs.

FBG rosette provides strain values close to the electrical one. When comparing the response of the three sensors individually, the response of the FBG at 0° appears to be the more precise. At the opposite, the higher difference was observed at 45°. The

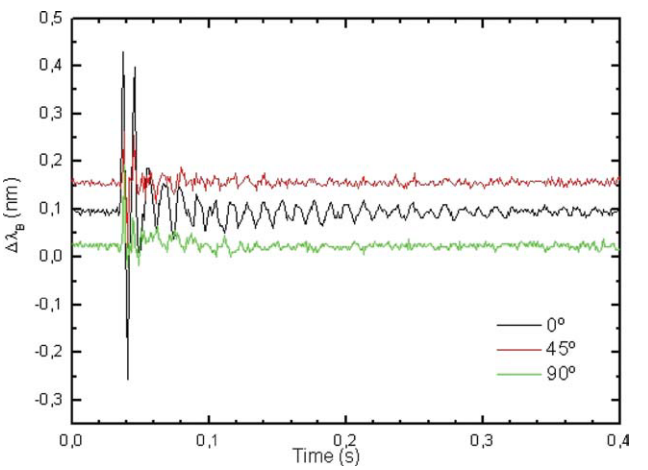

Figure 6 Dynamic response of the three FBG sensors. [Color figure can be viewed in the online issue, which is available at wileyonlinelibrary.com]

FBG were not significantly affected by any micobending imposed by the weaved reinforcement. No significant broadening of the reflection spectrum (i.e., variation of full width at half maximum (FWHM) in the range of 0.01 nm for an original width of 0.2 nm) were observed at the FBG reflection spectra along the test. The differences in the strain responses are though to be due to the strain transfer from the CFRP host composite to the FBG sensors. The observed difference is a limitation for the use of the CFRP strain rosette especially considering that for the higher strain values this error tends to decrease. The reproductivity of the CFRP rosette response was confirmed through repeated loadings.

4.2. Behavior in Flexion

The aluminium specimen was submitted to three-point bending tests. The rosette was placed at the opposite surface of load application. The test was implemented using the same testing machine. The displacement rate was set to 1 mm/min.

Figure 5 presents the response of the three FBG sensors. A good correlation between the electrical and optical sensors was verified. The same trend than for the tensile tests was observed, i.e., the higher response difference being observed for the FBG at 45°. This confirms that the worst alignment of this sensor with the reinforcement (compared with the sensors at 90° and 0°) at embedding results in a more complex strain transfer from the composite to the FBG. FBG sensors successfully measured the imposed bending strain as they were not exactly at the neutral line of the composite. The reproductivity of the CFRP rosette response to bending strain was also confirmed through repeated loadings.

4.3. Sensitivity to Vibration

The capability of the rosette to sense dynamic strain at low frequencies was verified from the impact of the aluminium sample by a noninstrumented hammer. One of the aluminium extremities was encastred, whereas the other remained supported. The acquisition rate of the BraggSCOPE was set to its maximum sampling rate (i.e., 10 kHz). In Figure 6 the variation of the central wavelength of the three FBG is presented. No comparison with the electrical strain rosette was possible due to the low maximal sampling rate of the data acquisition system used. The CFRP strain rosette can be considered for impact location from vibration measurement or from Lamb waves sensing in a similar approach as the one adopted by Betz et al. [19] using three rosettes. A high-speed interrogation procedure for FBG would however be necessary for Lamb waves sensing.

5. CONCLUSIONS

A thin and flexible CFRP delta strain rosette was implemented based on embedded FBG sensors. The interest of such strain rosette lies on its application at the surface of a structure. The low dimensions of this composite strain rosette significantly decrease its impact on the mechanical behavior of the structure. CFRP rosette proved to be competitive. The strain responses in the three directions were comparable with the response of the electrical strain rosette under tension and flexion solicitation. The less effective strain response, i.e., from the sensor at 45°, results of a more complex strain transfer at the host/sensor interface due to its worst alignment with the surrounding reinforcement. The range of application of this rosette is larger when compared to encapsulated optic and electric rosettes thanks to CFRP composite better long term properties. Besides, its CTE close to zero significantly decreases the effect of temperature on strain measurement. The sensitivity of FBG sensors at high frequencies permits the implementation of added capabilities such as damage location from triangulation using a network of rosettes.

ACKNOWLEDGMENTS

The authors would like to thank the Portuguese funding organisation Fundação para a Ciência e a Tecnologia (FCT) for financial support under the grant SFRH/BPD/41347/2007, to INESC-Porto for the optical fibre sensors and FiberSensing SA for the interrogation hardware.

REFERENCES

1. T. Valis, D. Hogg, and R.M. Measures, Fibre optic fabry – perot strain rosettes, Smart Mater Struct 1 (1992), 227–232.
2. T. Valis, D. Hogg, and R.M. Measures, Composite material embedded fiber optic fabry-perot strain rosette. Proc SPIE Fiber Opt Smart Struct Skins III 1370 (1990), 354–361.
3. S.W. Case, J.J. Lesko, B.R. Fogg, and G.P. Carman, Embedded extrinsic fabry-perot fiber optic strain rosette sensors. J Intell Mater Syst Struct 5 (1994), 412–417.
4. S. Magne, et al., Available at: www.ist.cea.fr/fr/programmes/capteurs/docs/fibre_optique/fiche_ produit_rosette_bragg1.pdf.
5. F.M. Haran, J.K. Rew, and P.D. Foote, Fiber Bragg grating strain gauge rosette with temperature compensation. Proc SPIE 3330 (1998), 220–230.
6. D.C. Betz, G. Thursby, B. Culshaw, and W.J. Staszewski, Advanced layout of a fiber Bragg grating strain gauge rosette. J Lightwave Technol 24 (2006), 1019–1026.
7. J. Matrat, K. Levin, and R. Jarlas, Implementation of a Bragg grating strain rosette embedded in composites. Proc SPIE 4328 (2001), 168–179.
8. Available at: http://www.smartfibres.com/Attachments/SmartPatch.pdf.
9. Available at: http:/www.fibersensing.com.
10. Y. Okabe, S. Yashiro, R. Tsuji, T. Mizutani, and N. Takeda, Effect of thermal residual stress on the reflection spectrum form fiber Bragg grating sensors embedded in CFRP laminates. Composites Part A 33 (2002) 991–999.
11. J.A. Guemes and J.M. Menéndez, Response of Bragg grating fiber-optic sensors when embedded in composite laminates. Compos Sci Technol 62 (2002), 956–966.
12. K.S.C. Kuang, R. Kenny, and M.P. Whelan, Embedded fibre Bragg grating sensors in advanced materials. Compos Sci Technol 64 (2001) 1379–1387.
13. R. de Oliveira, S. Lavanchy, R. Chatton, D. Costantini, V. Michaud, R. Salathé, and J-A.E. Månson, Experimental investigation of the effect of the mould thermal expansion on the development of internal stress during composite processing. Comp Part A 39 (2008), 1083–1090.
14. L. Tang, X. Tao, and C.-L. Choy, Effectiveness and optimization of fiber Bragg grating sensor as embedded strain sensor. Smart Mater Struct 8 (1999), 154–160.
15. C.A. Ramos, R. de Oliveira, and A.T. Marques, Design of an optical fibre sensor patch for longitudinal strain measurement in structures, Mater Design 30 (2009), 2323–2331.
16. D.A. Krohn, Fiber optic sensors: Fundamentals and applications. Instrument Society of America, 2000.
17. O. Frazão, N. Correia, C. Novo, A. Vieira, A.N. Costa, F. Araújo, and A.T. Marques, Optical fibre embedded in a composite laminate with applications to sensing. AEU - Int J Electron Commun 51 (1997), 1–5.
18. S. Magne, S. Rougeault, M. Vilela, and P. Ferdinand, State-of-strain evaluation with fiber Bragg grating rosettes: application to discrimination between strain and temperature effects in fiber sensors. Appl Opt 36 (1997), 9437–9447.
19. D.C. Betz, G. Thursby, B. Culshaw, and W.J. Staszewski, Structural damage location with fiber Bragg grating rosettes and lamb waves. Struct Health Monit 6 (2007), 299–308.